frontiers | Frontiers in Marine Science

TYPE Original Research
PUBLISHED 29 January 2025
DOI 10.3389/fmars.2025.1520497

OPEN ACCESS

EDITED BY
Kerstin Johannesson,
University of Gothenburg, Sweden

REVIEWED BY
Francisco Brusa,
National Scientific and Technical Research Council (CONICET), Argentina
Maël Grosse,
University of the Balearic Islands, Spain

*CORRESPONDENCE
Ting Sun
sunting@szu.edu.cn

RECEIVED 31 October 2024
ACCEPTED 06 January 2025
PUBLISHED 29 January 2025

CITATION
Feng L, Zhang S, Tao M, Sun T and Wang A (2025) Two new species of *Plagiostomum* (Prolecithophora, Plagiostomidae) from China with its morphology, phylogeny, and reproductive strategy.
Front. Mar. Sci. 12:1520497.
doi: 10.3389/fmars.2025.1520497

Two new species of *Plagiostomum* (Prolecithophora, Plagiostomidae) from China with its morphology, phylogeny, and reproductive strategy

Leyuan Feng[1], Shiyan Zhang[1], Ming Tao[2], Ting Sun[1]* and Antai Wang[1]

[1]Shenzhen Key Laboratory of Marine Bioresource and Eco-environmental Science, College of Life Science and Oceanography, Shenzhen University, Shenzhen, Guangdong, China, [2]Medical School, Shenzhen University, Shenzhen, China

Plagiostomum flatworms are small, free-living organisms frequently found in saltwater or freshwater habitats, but their biological characteristics remain largely unknown. Here, we describe two new species of *Plagiostomum* collected from the intertidal zone of the South China Sea, based on the integrative studies of morphology, phylogeny, reproduction, and juvenile development. Morphologically, *Plagiostomum nanhaiensis* sp. nov. can be distinguished from congeneric species by its three dark brown dorsal stripes, pear-shaped vesicula seminalis located ventrally to the intestine, and the testes surrounding the ovaries and bead-like sperm. Additionally, *Plagiostomum plagae* sp. nov. can be distinguished from *P. nanhaiensis* sp. nov. and other congeneric species by its two connected dorsal stripes, multiple spherical testes arranged along the ventral midline, a hemispherical vesicula seminalis located on the right ventral side, and grain-shaped sperm. Kimura's two-parameter distance and phylogenetic analyses further support the recognition of these two new species, showing that the three specimens of *P. nanhaiensis* sp. nov. and *P. plagae* sp. nov. form two separate clades within *Plagiostomum* with solid support. Moreover, these two new species exhibit similar habits and reproductive strategies, adopting hypodermic impregnation. The reproductive studies indicate that in natural environments or larger mating groups, these two new species tend to invest resources in male reproductive functions to enhance fertilization success, while in smaller or single-individual cultures, they shift resources toward complete female reproductive functions. Our results not only enrich the biodiversity data of the family Plagiostomidae in China but also provide new empirical evidence for existing sex allocation theories.

KEYWORDS

platyhelminthes, taxonomy, phylogeny, sex allocation, hypodermic impregnation

1 Introduction

Small free-living and hermaphrodite flatworms from the order Prolecithophora Karling, 1940, exhibit diverse morphologies and significant interspecies differences in regeneration and feeding habits and can be used for studies on speciation, evolution, cellular regeneration mechanisms, and ecological environments (Grosbusch et al., 2022; Wang et al., 2024). Prolecithophora comprises five families, which are further divided into 31 genera and 199 species (World List of Turbellarian Worms, 2024). The species of the genus *Plagiostomum* Schmidt, 1852, belonging to the family Plagiostomidae Graff, 1882, with 85 species described, are reported to inhabit diverse habitats from freshwater and brackish to marine (World List of Turbellarian Worms, 2024). However, the taxonomic and biodiversity studies of Prolecithophora remain largely unknown in China, with only three species (including an undescribed one) recorded (Gao et al., 2011; Ma et al., 2014; Wang et al., 2024).

Sex allocation refers to the assignment of resources to male or female reproduction, playing a crucial role in population survival, reproduction, and evolutionary trajectories (Vellnow et al., 2017, 2018). The sex allocation theories have developed from Charles Darwin's initial observations to Charnov and Fischer's foundational sex allocation theory, which explore how individuals balance reproductive functions in their reproductive investments to maximize their reproductive probability (Brand et al., 2022; Charnov, 1979, 1984; Fischer, 1981). Previous studies have suggested that genetic and environmental factors are crucial for sex allocation, such as cytonuclear conflict, mate availability, resource abundance, and competition intensity (Schärer and Pen, 2013; Vellnow et al., 2017, 2018). However, previous sex allocation studies of flatworms have primarily focused on the genus *Macrostomum* (Macrostomorpha, Macrostomidae) while little attention paid to prolecithophorans, highlighting the requirement of sex allocation investigation of this order (Giannakara and Ramm, 2017; Janicke et al., 2013, 2016; Ramm, 2017).

Accurately measuring sex allocation in hermaphroditic organisms poses significant experimental challenges and requires verification of their alignment with theoretical models (Schärer, 2009). In gonochoristic species, sex allocation is typically measured through offspring sex ratios (Schärer, 2009). However, in hermaphrodites, it is more complex due to the need to quantify both male and female organs, considering static and dynamic changes over time (Schärer, 2009). Flatworms of the order Macrostomida are emerging model organisms for sex allocation studies in hermaphroditic animals due to their transparent bodies, which are beneficial for the direct observation and measurement of the relative changes in the size of the testes, ovaries, and vesicula seminalis. However, the sex allocation assessment of these species is usually based on the proportions of the male and female organs and glands (Brand et al., 2022; Janicke et al., 2013; Vellnow et al., 2018).

Understanding the reproductive strategies of these organisms, including their mating behaviors, is crucial for comprehensively assessing sex allocation. Previous studies have identified hypodermic impregnation as a significant mating strategy observed in Prolecithophora and Macrostomorpha species, involving the direct injection of simplified sperm into the partner's body (Brand et al., 2022; Schärer et al., 2004; Wang et al., 2024). This process often results in local sperm competition and can drive a differential allocation of reproductive resources between male and female functions (Giannakara and Ramm, 2017; Janicke et al., 2016). Notably, *Macrostomum* exhibits two mating strategies—hypodermic impregnation and reciprocal copulation—with the latter involving complex sperm exchange and promoting balanced investment in both reproductive roles (Brand et al., 2022; Schärer et al., 2004, 2011). Although a study has observed the hypodermic impregnation behavior and individual developmental process of *Plagiostomum robusta* (Wang et al., 2024), the sex allocation and reproduction of prolecithophorans remain largely unknown.

We collected over 500 flatworm specimens from the intertidal zone of the South China Sea. Our preliminary analyses showed that they belong to two new species of the genus *Plagiostomum*. Therefore, the aims of the study were to 1) describe two new species of *Plagiostomum*, 2) determine the genetic distances and phylogenetic position of the new species, and 3) clarify their habits, sex allocation, and reproduction. Our discovery will enhance the biodiversity study of prolecithophorans in China and provide new empirical evidence for the extreme forms of sex allocation.

2 Materials and methods

2.1 Specimen collection

The specimens were collected from Yanzhou Lijie Pier, Huizhou, Guangdong Province, China (22°43′12″N, 114°57′36″E), with a water temperature of 24°C, pH of 7.59, and salinity of 32‰ (Supplementary Figure S1). Briefly, the flatworms attached to submerged rocks and oyster shells were rinsed in a water bucket and filtered using 200-mesh, 160-mesh, and 40-mesh plankton nets.

2.2 Cultivation and observation

The flatworms were cultured in a 10-cm-diameter round buckle box with the addition of habitat sediment, wheat grains, and protozoa. The water was changed every 3 days, with the salinity maintained at 30‰ and the water temperature at 23°C ± 2°C. The behaviors of the flatworms, including movement, predation, mating, and spawn, were observed and recorded under an Olympus SZX16 stereomicroscope. The eggs were transferred to a clean culture dish for the continuous observation of embryonic development, hatching, and juvenile development under Olympus BX51 in conjunction with the Olympus DP72 camera system.

2.3 DNA extraction, amplification, and sequencing

Three flatworms starved for 2 days were treated with liquid nitrogen for 15 s, and DNA was extracted using the E.Z.N.A.

Mollusc DNA Kit (Omega, Norcross, GA, USA). PCR amplification was conducted using Vazyme 2×Taq Plus MasterMix II (Dye Plus). For the primers and procedures for amplifying *18S rDNA* and *28S rDNA*, refer to Wang et al. (2024). After quality examination using 1.2% agarose gel electrophoresis, the PCR products were sequenced in Tsingke Biological Technology (Beijing, China).

2.4 Phylogenetic analysis

The *18S rDNA* and *28S rDNA* fragments of the 21 Plagiostomidae species [all molecular data currently available for Plagiostomidae species in National Center for Biotechnology Information (NCBI)] and two species of *Rogneda* Uljanin, 1870, as the outgroup were obtained from GenBank (https://www.ncbi.nlm.nih.gov/) (Supplementary Table S1). Multiple sequence alignments were performed using MAFFT on the online server (https://mafft.cbrc.jp/alignment/server/) with the Q-INS-i algorithm and default parameters (Kuraku et al., 2013; Katoh et al., 2019), and sequence trimming was conducted using trimAl v1.2rev57 with the -automated1 parameter (Capella-Gutierrez et al., 2009). Base substitution saturation was tested using DAMBE v5.3.19 (Xia, 2013). The Concatenation Sequence program (Vaidya et al., 2011) in the PhyloSuite v1.2.3 (Xiang et al., 2023) was used to merge the *18S rDNA* and *28S rDNA* sequences of each species.

ModelFinder v2.2.0 (Kalyaanamoorthy et al., 2017) was used to select the best-fit substitution models for the *18S rDNA* and *28S rDNA* datasets using the Akaike information criterion (AIC) method (Lanfear et al., 2012): GTR+F+I+R3 (for *18S rDNA*) and GTR+F+I+R4 (for *28S rDNA*) for IQ-TREE; both datasets used GTR+F+I+G4 for MrBayes. IQ-TREE v1.6.2 (Nguyen et al., 2015) was used to construct the maximum likelihood (ML) phylogenetic tree using 1,000 ultrafast bootstrap replicates. MrBayes ver. 3.2.7a (Ronquist et al., 2012) was used to construct the Bayesian inference (BI) phylogenetic tree, employing the Markov chain Monte Carlo (MCMC) algorithm with four simultaneous chains, running for 2,000,000 generations, sampling every 1,000 generations, and discarding 25% of the burn-in samples. The average standard deviation of split frequencies was less than 1%. TRACER v1.7.1 (Rambaut et al., 2018) was used to check the.p files from each run, ensuring that all parameters had an effective sample size (ESS) greater than 200. The phylogenetic tree results were visualized using Figtree v1.4.3 (Rambaut, 2009).

2.5 Sex allocation experiment and paraffin sections

To study the reproduction of the new species, 12 single-individual cultured groups, 10 three-individual cultured groups, and a population cultured group were established. Mature flatworms (larger than 600 μm in length) in the single-individual cultures were reared in six-well cell culture plates (well diameter 35 mm). The three individual cultured groups were conducted on a small scale in 90-mm glass evaporation dishes, while the population cultured group consisted of 200–300 mature flatworms in a 10-cm-diameter round buckle box. Habitat water and food were supplied daily. Flatworms at different cultured stages were fixed using Bouin's fluid and then washed and soaked in 75% ethanol until the epidermis was transparent and the shadow of the copulatory apparatus was visible. The presence or absence of male copulatory apparatus was examined under an Olympus SZX16 stereomicroscope. Paraffin tissue sections were then prepared to observe the changes in the copulatory apparatus according to Yang et al. (2020). Additionally, 60 sexually mature flatworms freshly collected from the habitat were used as controls.

2.6 Abbreviations used in the figures

b. brain, ca. common atrium, cvd. common vitelline duct, dp. distal penis, ds. distal sac, e. eye, eg. egg, fg-1. frontal gland-1 (orange-staining frontal gland), fg-2. frontal gland-2 (aniline blue-staining frontal gland), gg. gonopore gland, go. gonopore, in. intestine, m. mouth, o. ovary, p. pharynx, pg. prostate gland, pp. penial papilla, prp. proximal penis, ps. penile sheath, s. sperm, sg. shell gland, t. testis, v. vitellaria, va. vagina, vd. vitelline duct, vs. vesicula seminalis.

3 Results

3.1 Systematics

Order: Prolecithophora Karling, 1940;
Family: Plagiostomidae Graff, 1882;
Genus: *Plagiostomum* Schmidt, 1852;

3.1.1 *Plagiostomum nanhaiensis* sp. nov.

Material examined. Holotype: PLA-Pl010, sagittal sections on 42 slides. Paratypes: PLA-Pl011, horizontal sections on 26 slides; PLA-Pl012, horizontal sections on 26 slides; PLA-Pl013, sagittal sections on 30 slides; PLA-Pl014, transverse sections on 75 slides. Sex allocation experiment specimens: PLA-Pl015, sagittal sections on 20 slides; PLA-Pl016, sagittal sections on 26 slides; PLA-Pl017, horizontal sections on 26 slides; PLA-Pl018, whole mount; PLA-Pl019, whole mount.

Distribution. Currently only found in the estuary river near Yanzhou Lijie Pier, Huizhou, Guangdong Province, China.

Etymology. The epithet "*nanhaiensis*" refers to the location of this species, the South China Sea, in Chinese (Nanhai).

Diagnosis. *Plagiostomum* species with three stripes of markings on the dorsal surface, tail stripe extending to the dorsal side of the gonopore and forming an inverted triangle.

Description. Body length up to 1.2 mm (n = 10), width 0.21 to 0.34 mm (n = 10, Figures 1A, B). Body cylindrical, head rounded, and tail slender and transparent (Figure 1A). Dorsal surface with three pigmentation stripes: a semicircular head stripe between the eyes and snout, a dark brown transverse band at mid-body, and a

10.3389/fmars.2025.1520497

tail stripe extending to the gonopore (Figures 1A–C). Ventral surface without pigmentation. A concave glandular pit situated between the snout and brain. Pit contains two frontal glands: frontal gland-1 (fg-1), orange-yellow staining, and frontal gland-2 (fg-2), aniline blue staining (Figures 1D, E, 2C, M). Fg-1 consists of 4–7 fine ducts, fg-2 positioned medially with 4–12 ducts, both leading from the pit to the exterior (Figures 1D, E, 2C, M). Eyes paired, interocular distance 60–70 μm (n = 3, Figures 1A–D). Brain posterior to the eyes. Frustum-shaped pharynx posterior to the brain, with the anterior part slanting toward the mouth and the posterior part connecting to the intestine (Figures 1D, 2A, D, M). The pharynx lacks complex musculature or foldability and contains

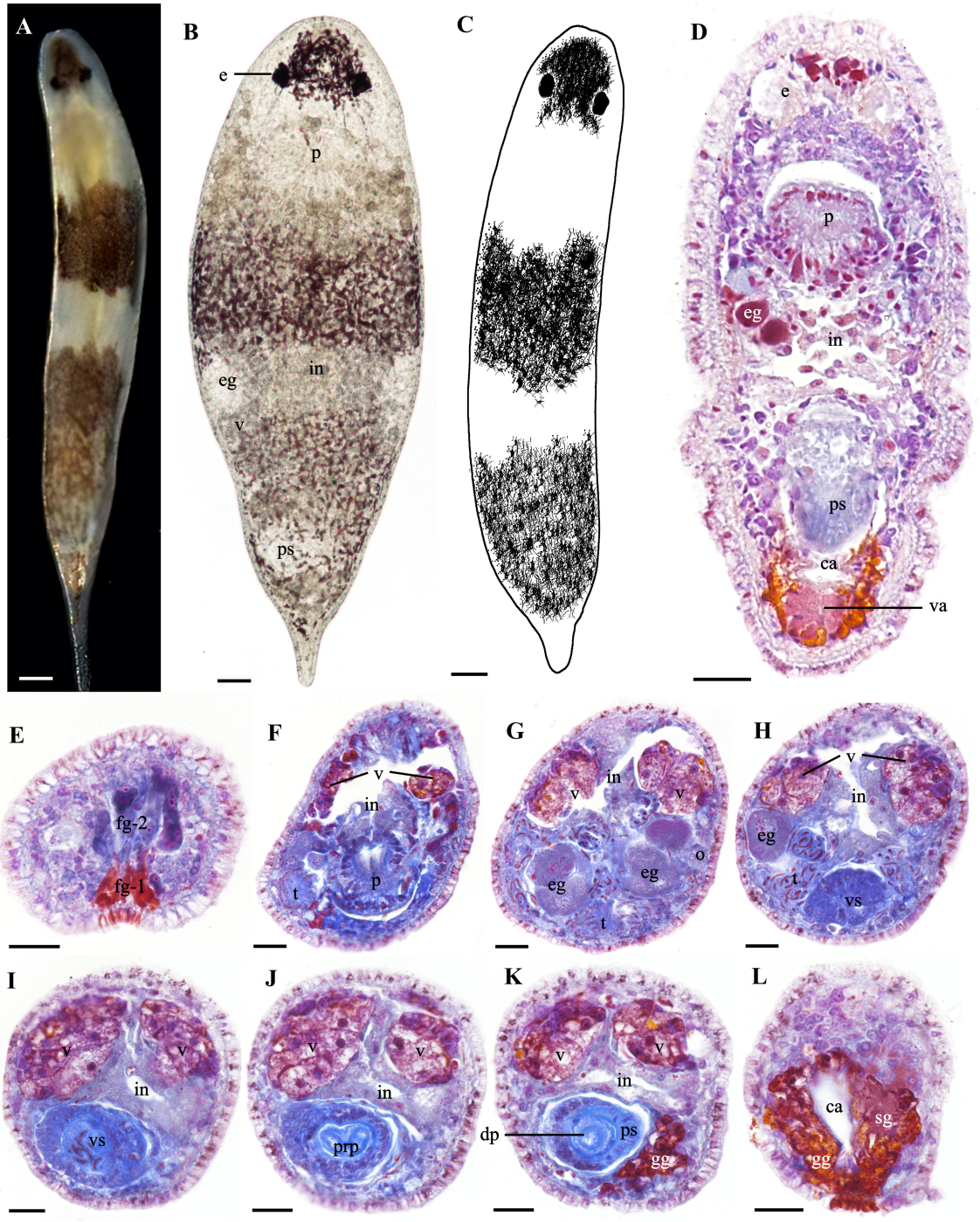

FIGURE 1
Morphology and histology of *Plagiostomum nanhaiensis* sp. nov. **(A)** Dorsal view of the live specimen. **(B)** Flattened morphology of the live specimen. **(C)** Patten of dorsal view. **(D)** Horizontal section. **(E–L)** Transverse sections. **(E)** Structure of the frontal glands in the head. **(F)** Distribution of testes and ovaries on both sides of the pharynx. **(G)** Morphology of the testes and sperm surrounding the oocytes. **(H)** Distribution of sperm around the vesicula seminalis. **(I)** Morphology of the vesicula seminalis. **(J)** Morphology of the distal penis and distal sac. **(K)** Morphology of the proximal penis and penile sheath. **(L)** Gland distribution in the common atrium and vagina. **(A–D)** Scale bar, 50 μm. **(E–L)** Scale bar, 25 μm.

10.3389/fmars.2025.1520497

cilia within its lumen (Figures 2D, M). Granular pharyngeal gland cells surround the base of the pharynx (Figures 1D, F). Intestine is straight and unbranched, extending from the posterior end of the pharynx to above the common atrium (Figures 2A, M).

Paired vitellaria symmetrically distributed along two sides of the dorsal body, extending from two sides of the pharynx to the anterior of the vagina (Figures 1F–K, 2A, B, E–G, L). Multiple vitelline ducts converge into the common vitelline duct (Figures 2B, E, F, L). Paired ovaries distributed on two sides of the ventral body, without an enclosing membrane (Figures 1G, 2B, L). Mature follicles positioned at the posterior end of the ovaries. As egg follicles migrate dorsally, oocytes gradually enlarge and connect with the vitellaria and common vitelline duct (Figures 2B, E, F, L). Oocytes migrate via the common vitelline duct to the vagina and then to the common atrium (Figures 2E–G, L). Vagina short, surrounded by shell glands, with its distal end opening into the common atrium (Figures 1D, L, 2G, L–M).

Testes in the ventral body without a sac-like structure. In cross-sections, mature sperm appear as long, segmented structures resembling a chain of beads, enveloped by a thin membrane (Figures 2H, I). Testes and their surrounding sperm are distributed on both sides of the pharynx and ventral side of the intestine,

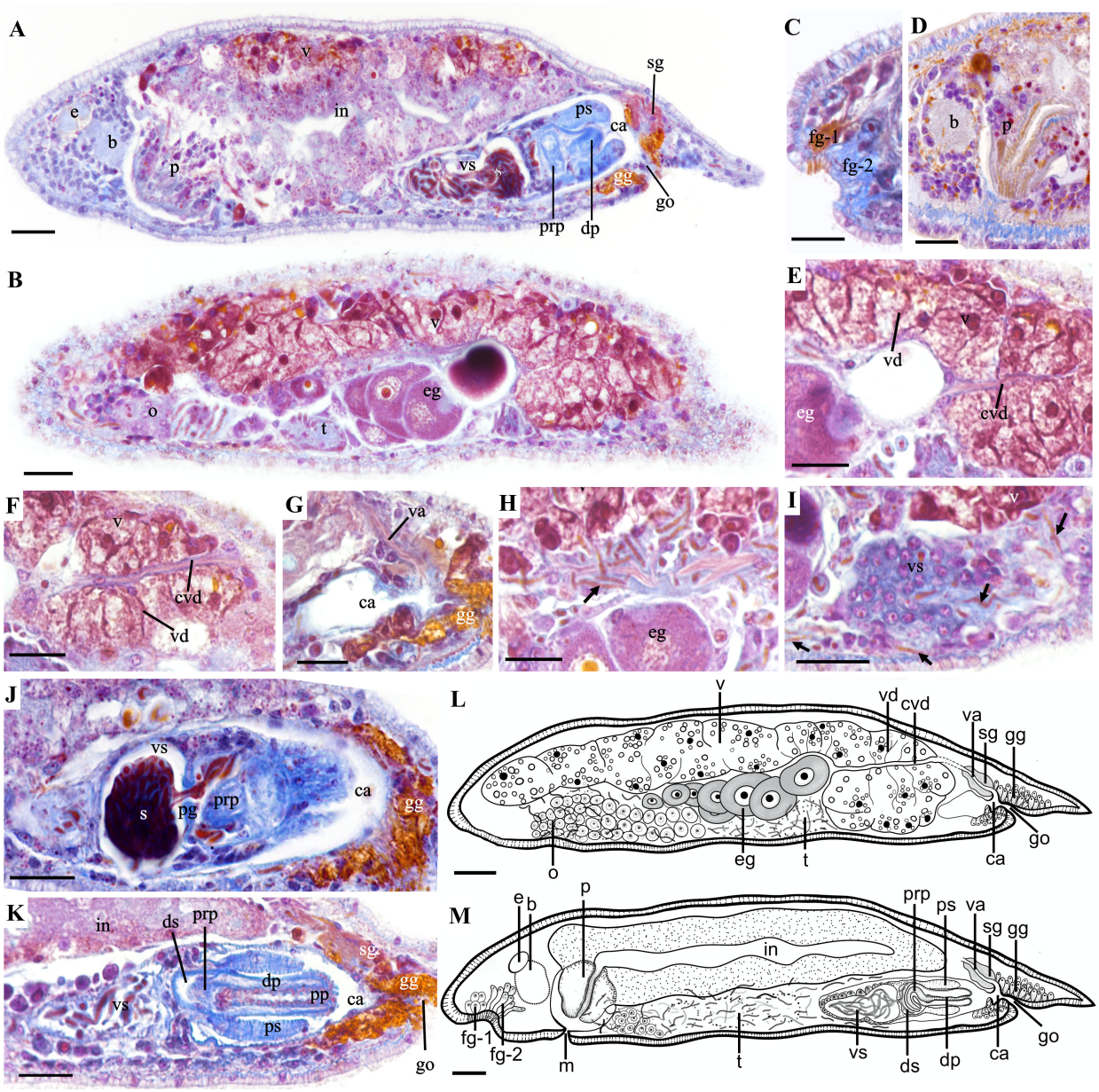

FIGURE 2
Sagittal sections and biological illustration of *Plagiostomum nanhaiensis* sp. nov. **(A, B)** Overall sagittal section. **(C, D)** Head structures. **(E, F)** Morphology of the vitellaria and common vitelline duct, with oocytes migrating from the ovary to the common vitelline duct. **(G)** Structure of the common atrium and vagina. **(H, I)** Distribution and direction of sperm. Arrows: sperm. **(J, K)** Structure of the male reproductive organs. **(L)** Sagittal view of both sides of the body. **(M)** Sagittal view of the middle part of the body. Scale bar, 25 µm.

surrounding the ovaries (Figures 1F–H, 2B, M). Sperm migrate posteriorly from the region around the ovaries along vitellaria and body wall, eventually entering vesicula seminalis from its posterior end (Figures 2H, I). Additionally, a few sperm were found in the brain, pharynx, and intestinal epithelium; however, it was impossible to determine their origin, whether from the individual itself or its mate. Vesicula seminalis pear-shaped, ventrally in the mid-posterior region of the intestine (Figures 1H, I, 2A, I–K, M). Vesicula seminalis surrounded by thick glandular cells and contains numerous sperm (Figures 1H, I, 2I, K, M). Vesicula seminalis opens posteriorly toward the distal sac, which houses a built-in prostate gland (Figures 2J, M). Distal sac narrow and hemispherical, with its posterior end connecting to the penis and penile sheath (Figures 2J, K, M). Thickness of the penile sheath similar to the diameter of the penis, approximately 9 µm (n = 3, Figures 1K, 2A, K, M). Penis consists of a proximal penis, a distal penis, and penial papilla. Proximal penis coiled inside distal sac; distal penis slender and tubular, encased by the penile sheath. Musculature thickens at the penial papilla, exposed in the common atrium and toward the gonopore (Figure 2K). Common atrium situated between the penis and gonopore, communicating with the gonopore (Figures 2A, G, J–M). Gonopore opens ventrally near the posterior end of the body, surrounded by a dense arrangement of gonopore glands (Figures 1D, L, 2K).

Remark

The special dorsal stripes of *P. nanhaiensis* sp. nov. and *Plagiostomum plagae* sp. nov. represent a distinctive feature that helps differentiate them from other congeneric species. *P. nanhaiensis* sp. nov. is the most similar to *Plagiostomum vittatum* and *Plagiostomum abboti* Karling, 1962, in dorsal stripes and body sizes (Frey and Leuckart, 1847; Karling, 1962; Tyler et al., 2006-2024). However, the stripes of *P. vittatum* are reddish-brown or magenta, and its male copulatory apparatus is located in the posterior part of the intestine on the right side of the body, with the vesicula seminalis surrounded by the intestine (Frey and Leuckart, 1847; Tyler et al., 2006-2024). In contrast, the stripes of *P. nanhaiensis* sp. nov. are brownish-black or brown, and its male copulatory apparatus is located in the ventral part of the intestine along the central axis (Figures 1D, H–K) showing significant differences from *P. vittatum*. The tail pattern of *P. abboti* consists of horizontal stripes, and its sperm is short, with rounded head and pointed tail. Additionally, its vesicula seminalis frontly connects to the testes with a long duct (Karling, 1962). In *P. nanhaiensis* sp. nov., the tail stripes extend to the tail tip and form an inverted triangle, and its sperm is long and segmented like beads. Furthermore, no duct or opening was observed at the anterior end of the vesicula seminalis in *P. nanhaiensis* sp. nov.; instead, sperm entered from the posterior end of the vesicula seminalis (Figure 2I).

Behavioral characteristics and feeding habits. *P. nanhaiensis* sp. nov. prefers to inhabit areas with muddy substrates around plant roots and beneath with organic debris. The worms will quickly avoid each other during encounters. During laboratory cultivation, the worms feed on protozoa and exhibit rapid feeding behavior toward cooked egg yolk and locust ovarian granules. However, their intestines will rupture if the food particles are too large or tough. Additionally, *P. nanhaiensis* sp. nov. can partly prey on brine shrimp juveniles while its normal growth and reproduction requirements cannot be satisfied. Notably, *P. nanhaiensis* sp. nov. exhibits cannibalistic behavior during co-cultivation, while coexisting with the species from Rhabdocoela for a long period. By contrast, *P. nanhaiensis* sp. nov. is often preyed upon by Macrostomorpha species during co-cultivation.

Oviposition behavior and ontogenetic process. *P. nanhaiensis* sp. nov. exhibits a preference for spawning in areas with abundant debris. In the initial stage of spawning, its body contracts into a gourd shape, while mucus is extruded from the gonopore, adhering to the bottom of the dish and subsequently hardening in contact with water to form a stable base (Figure 3A). By contrast, when situated in open or well-lit environments, the worm utilizes its tail as a pivot to oscillate vertically, employing its head to transport lateral debris to the vicinity of the oviposition site, thereby providing partial concealment for the eggs (Figure 3A). During this period, a slight increase in the expansion of the tail end is observed, with the outlines of the eggs becoming distinctly visible (Figure 3A). Subsequently, the worm extends its body forcefully, elevating the gonopore, and a string-like egg stalk extends upward from the center of the base, with the egg being extruded and adhered to the stalk. The egg is attached to the wall of the dish via the egg stalk and base. Initially, the collective morphology of the base, egg stalk, and eggs resembles that of a wine goblet (Figure 3B). Approximately 4 minutes later, the eggshell transitions to a light brown color, and after 28 minutes, it appears dark brown (Figure 3B). After the accomplishment of spawning, the worm collects some debris to cover its eggs before leaving if the surrounding area is exposed.

We recorded the developmental process of 130 eggs of *P. nanhaiensis* sp. nov., and we observed that the hatching period ranged from 3 to 7 days, with two to six juveniles hatching from each egg. On the first day after oviposition, the eggs are filled with contents that are irregularly distributed. By the second day, distinct embryos appear within the eggs, with visible cavities in the eggshell. Subsequently, the embryos undergo differentiation and development, with structures such as the intestine gradually emerging (Figure 3C). During this period, embryonic proliferation occurs, with volume increasing and the entire embryo slightly expanding (Figure 3C). One day before hatching, the juveniles are completely developed in the egg with visible eye spots (Figure 3C). The newly hatched juveniles are devoid of patterns, exhibiting a grayish-white translucent appearance, with body lengths between 0.24 and 0.28 mm (n = 3). Approximately 5 days later, brown stripes emerge on the snout and dorsal side of the body, and the pharynx gradually develops. By the 15th day, brown pigmentation begins to appear on the tail, and with the development, the pigmentation deepens to a dark brown coinciding with an increase in body length (Figure 3D).

3.1.2 *Plagiostomum plagae* sp. nov.

Material examined. Holotype: PLA-Pl020, sagittal sections on 25 slides. Paratypes: PLA-Pl021, sagittal sections on 36 slides; PLA-Pl022, transverse sections on 42 slides. Sex allocation experiment specimens: PLA-Pl023, whole mount; PLA-Pl024, sagittal sections on 24 slides; PLA-Pl025, sagittal sections on 16 slides; PLA-Pl026, sagittal sections on 15 slides.

10.3389/fmars.2025.1520497

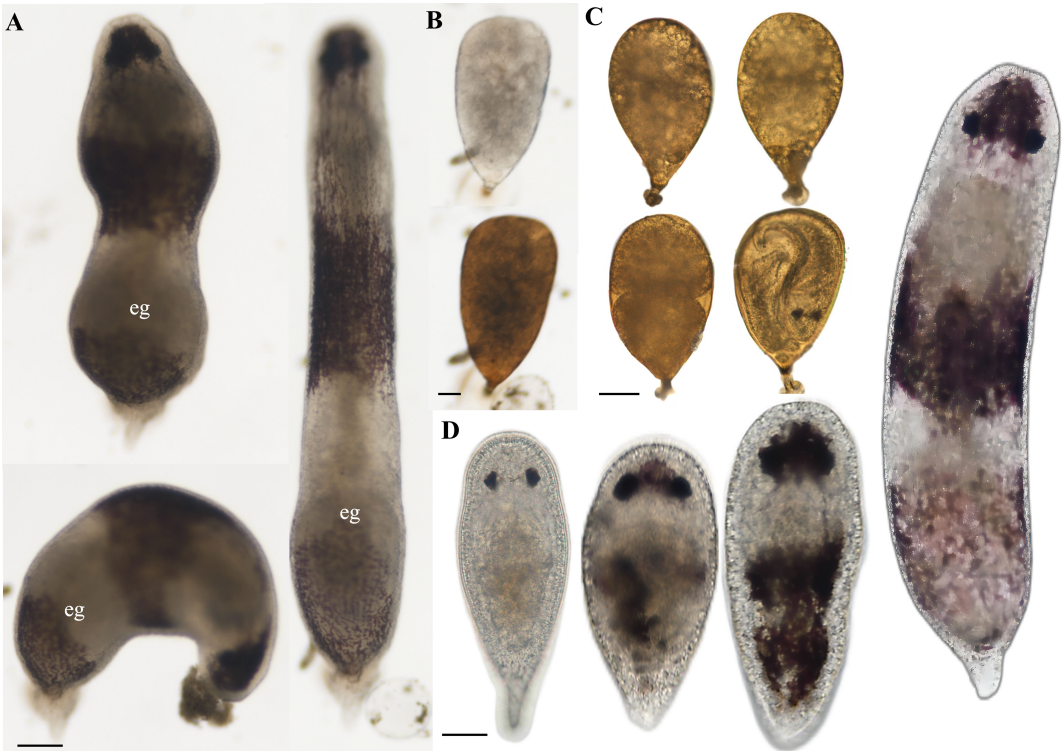

FIGURE 3
Oviposition process and developmental process of the embryos and juveniles of *Plagiostomum nanhaiensis* sp. nov. **(A)** Oviposition process. **(B)** Egg color change phenomenon. **(C)** Development of the embryos in egg. **(D)** Living specimens at different developmental stages. **(A)** Scale bar, 100 µm. **(B–D)** Scale bar, 50 µm.

Distribution. Currently only found in the estuary river near Yanzhou Lijie Pier, Huizhou, Guangdong Province, China.

Etymology. The epithet "*plagae*" is derived from the Latin word "*plaga*", meaning "stripe", which refers to the two prominent stripes on the dorsal surface of this species.

Diagnosis. *Plagiostomum* species with two obvious dark stripes on the dorsal surface, multiple spherical testes arranged in series along the ventral midsection of the body, the semi-elliptical vesicula seminalis located on the right ventral side of the intestine, and a nipple-shaped penis enclosed by the penile sheath.

Description. Body length up to 1.2 mm (n = 5). Head rounded, body cylindrical, width approximately 0.1 to 0.23 mm (n = 5, Figure 4A). Dorsal surface with two dark brown stripes. Head stripe extending from the eyes to the tip of the snout, formed by reticulated pigment cells (Figures 4A, B). Dorsal midsection with semicircular stripe connecting to vertical reticulated brown stripe at posterior end (Figures 4A, B). Tail conical and milky white (Figure 4A). A concave glandular pit between the snout and brain, composed of frontal gland-1 (fg-1), stained orange-yellow, and frontal gland-2 (fg-2), stained aniline blue (Figures 4C, 5A, C, J). Fg-1 consists of five to seven fine glandular ducts (in cross-section) extending from pit to exterior end, while fg-2 is medially located to fg-1 with four to seven fine ducts (in cross-section) extending from pit to exterior end (Figure 5A). Paired eyes composed of three pigment cells, interocular distance 40 to 60 µm (n = 3, Figures 4A, B). Brain posterior to the eyes. Conical pharynx posterior to the brain, with the anterior part slanting toward the mouth and the posterior part connecting to the intestine (Figures 5B–D). The pharynx contains cilia within its lumen (Figures 5B, D, J). Pharyngeal gland cells surround the pharynx (Figures 5B–D).

Paired vitellaria distribute along the dorsolateral intestine, above extending from the pharynx to the common atrium (Figures 5C, D, J). Paired ovaries distributed along the ventrolateral sides of the intestine. Mature oocytes migrate dorsally from the ventral side and connect with vitellaria (Figures 5C, E). Oviducts not observed. Vagina short, with its distal end opening into the narrow common atrium, surrounded by shell glands (Figures 5H–J).

Multiple spherical testes arranged in series along the ventral midsection without visible sperm ducts (Figures 4C, 5D, J). Mature sperm grain-shaped, concentrated within the testes, with a few migrating to the brain and epidermis (Figures 5D, F, G). Hemispherical vesicula seminalis located on the right side of the ventral midsection, with its wall surrounded by gland cells (Figures 4C, 5F, H, I). It contains clumps of sperm, and a prostate gland is present near the opening to the distal sac (Figures 4C, 5F, H, I). Distal sac spherical, connecting with penis and penile sheath. Penis nipple-shaped, with a longer proximal end coiled inside the distal sac (Figures 5H, I). Distal end and penial papilla covered by penile sheath, opening into the common atrium (Figure 5H). Common atrium a γ-shaped, elongated tube, extending toward the ventral side and leading to the gonopore (Figures 5C, H–J). Gonopore opens on the ventral side near the posterior body end, surrounded by numerous gonopore glands (Figures 5C, H–J).

10.3389/fmars.2025.1520497

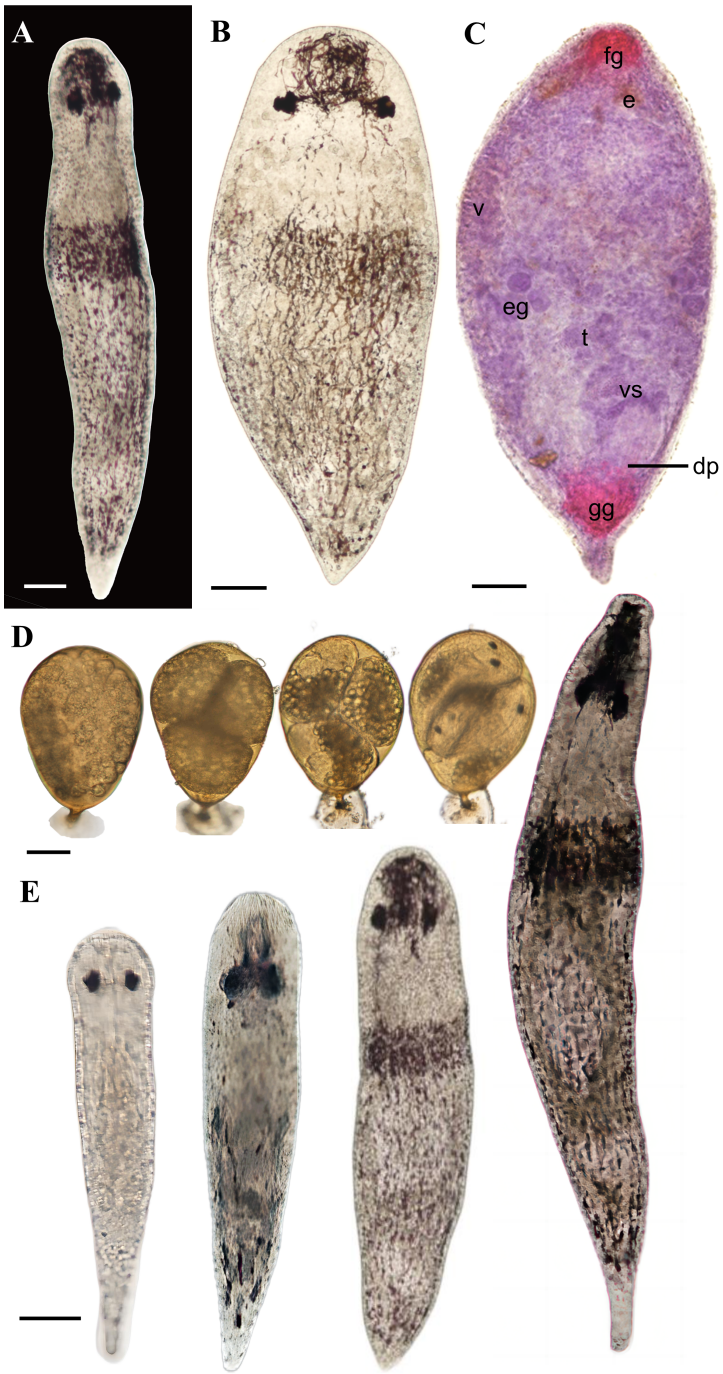

FIGURE 4
Live specimen of *Plagiostomum plagae* sp. nov. **(A)** Dorsal view of the live specimen. **(B)** Flattened morphology of the live specimen. **(C)** Whole mount. **(D)** Development of the embryos in egg. **(E)** Living specimens at different developmental stages. Scale bar, 50 µm.

Remarks

P. plagae sp. nov. is morphologically similar to *Plagiostomum koreni* Jensen, 1878, in the mid-body transverse stripes, following scattered vertical stripes, and penis inclined dorsally (Jensen, 1878). In *P. koreni*, the testes are paired and located on both sides of the posterior body, with the middle of the vesicula seminalis connecting to the vas deferens, forming a simple, elongated tubular structure (Jensen, 1878). By contrast, in *P. plagae* sp. nov., the spherical testes are arranged in a series along the central axis, and no vas deferens-like structure is observed, showing significant differences from *P. koreni*. Therefore, these morphological differences strongly support *P. nanhaiensis* sp. nov. and *P. plagae* sp. nov. as a new species of *Plagiostomum*. In addition, *P. plagae* sp. nov. can be distinguished from *P. nanhaiensis* sp. nov. by differences in external morphology and reproductive structures. The mid-body ring and tail stripes of *P. nanhaiensis* sp. nov. are separated, while the mid-body ring stripe of *P. plagae* sp. nov. connects with the reticulated vertical stripes on the posterior end. Additionally, the male copulatory apparatus of *P.*

10.3389/fmars.2025.1520497

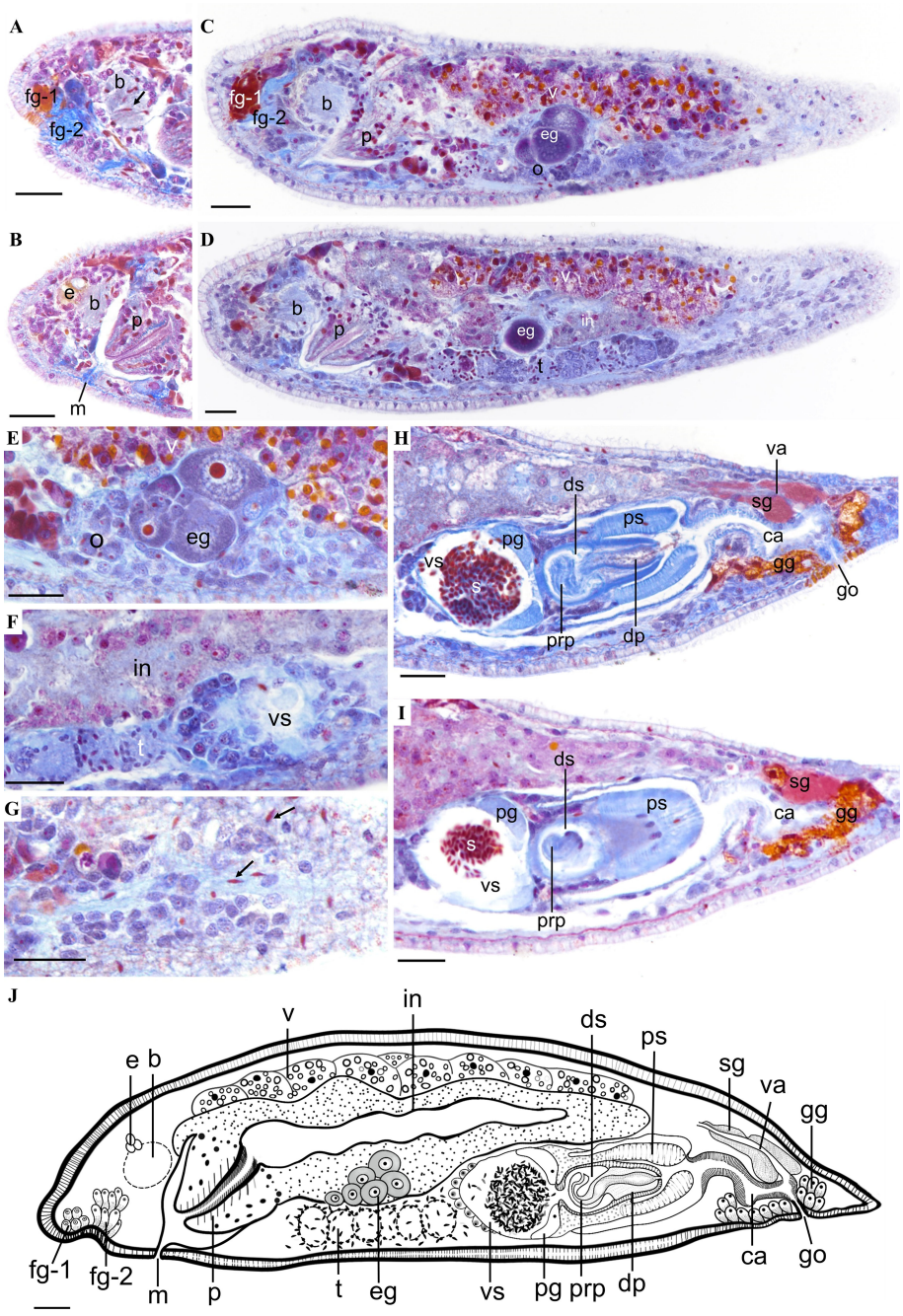

FIGURE 5
Sagittal sections and biological illustration of *Plagiostomum plagae* sp. nov. **(A)** Structure of the frontal gland and brain, with free sperm present in the brain. **(B)** Pharyngeal structure. **(C)** Relative position of the female reproductive organs. **(D)** Relative position of the testes. **(E)** Ovaries and oocytes. **(F)** Morphology of the testes. **(G)** Distribution of free sperm. **(H, I)** Structure of the male reproductive organs. Arrows: free sperm within the body. **(J)** Reconstruction of the reproductive structures. Scale bar, 25 µm.

nanhaiensis sp. nov. is in the central axis of the body, with a pear-shaped vesicula seminalis, and the prostate gland is embedded within the distal sac wall. In contrast, those of the latter are positioned on the right side, containing a semi-elliptical vesicula seminalis with the prostate gland situated inside it. The testis distribution also differs significantly: in the former, they are diffusely spread from the mid-ventral side to both sides, surrounding the ovaries and oocytes, while in the latter, they are spherical, arranged in a series, and confined to the mid-ventral region. Sperm of the former is long and bead-like, while it is short and grain-shaped in the latter. Meanwhile, when *P. nanhaiensis* sp. nov. and *P. plagae* sp. nov. were reared together, no hybridization behavior was observed. These results fully supported that they are two distinct species.

Behavioral characteristics and feeding habits. During cultivation, *P. plagae* sp. nov. prefers to inhabit the sides of containers and often floats on the water surface, rarely contacting others. By contrast, this species usually quickly turns away when

encountering another individual during movement. Its feeding habits are similar to those of *P. nanhaiensis* sp. nov., including consuming egg yolk, locust ovaries, brine shrimp juveniles, and protozoa.

Ontogenetic process. We recorded the hatching process based on 15 eggs of *P. plagae* sp. nov., of which 81.8% hatched. The hatching period ranged from 4 to 6 days, and one to four juveniles hatched from an egg. The hatching process was similar to that of *P. nanhaiensis* sp. nov. (Figure 4D). Newly hatched juveniles were translucent grayish white, with body lengths from 0.31 to 0.34 mm ($n = 3$, Figure 4E). After 4 to 5 days, pigmentation appeared between the eyes and on the snout, and longitudinal stripes developed on the dorsal side, with the juvenile development, the dorsal stripes increased, and a ring band formed around the midsection (Figure 4E).

3.2 Genetic distance and phylogenetic analyses

The amplified *18S rDNA* and *28S rDNA* sequences of the two species range from 1,600 to 1,700 bp in length. After alignment and trimming, the lengths of each dataset were 1,753 bp (*18S rDNA*), 1,478 bp (*28S rDNA*), and 3,233 bp (concatenated dataset), with low base substitution saturation (ISS < ISS.c), making them suitable for phylogenetic tree construction. The Kimura two-parameter (K2P) distance between the two new species and *Plagiostomum morgani* Graff, 1911, is the shortest among *Plagiostomum* species, ranging from 5.3% to 6.5%. The ML and BI phylogenetic trees constructed from the three datasets had consistent topologies. Three individuals of *P. nanhaiensis* sp. nov. and *P. plagae* sp. nov. formed independent clades with solid support in both BI (posterior probability = 1.00) and ML (bootstrap value = 100) analyses, being sister to each other (Figure 6). The clade of two new species clustered with *Plagiostomum* sp. SL-2020 and *P. morgani* Graff, 1911, close to the clade comprising *P. vittatum* Jenssen, 1878, *Vorticeros auriculatum* Müller, 1784, and *Vorticeros ijima* Tozawa, 1918. These results further supported the recognition of these two new species.

3.3 Mating behavior of the two new species

Our observation revealed that the two new species employed hypodermic impregnation as their fertilization model. Notably, self-fertilization was documented in both species during individual cultivation. In this instance, the tail curls upward, and the reproductive organ injects itself near the head and pharyngeal region. In contrast, triad and group cultivation facilitated cross-fertilization among these two species. Remarkably, we observed self-fertilization of *P. nanhaiensis* sp. nov. on two occasions when other conspecifics were present, suggesting that self-fertilization is not restricted to individual cultivation.

The mating behavior analysis in six pairs of *P. nanhaiensis* sp. nov. revealed that individuals engage in head-to-head contact before fertilization to assess each other. Following the initial interaction, both individuals rapidly curl up and separate. In scenarios involving multiple individuals, they may extend their copulatory organs; however, once one individual successfully inserts its copulatory organ subcutaneously into another, the remaining individuals retract their penises. During mating, the penis of the injecting individual protrudes from the gonopore (Figure 7A), and

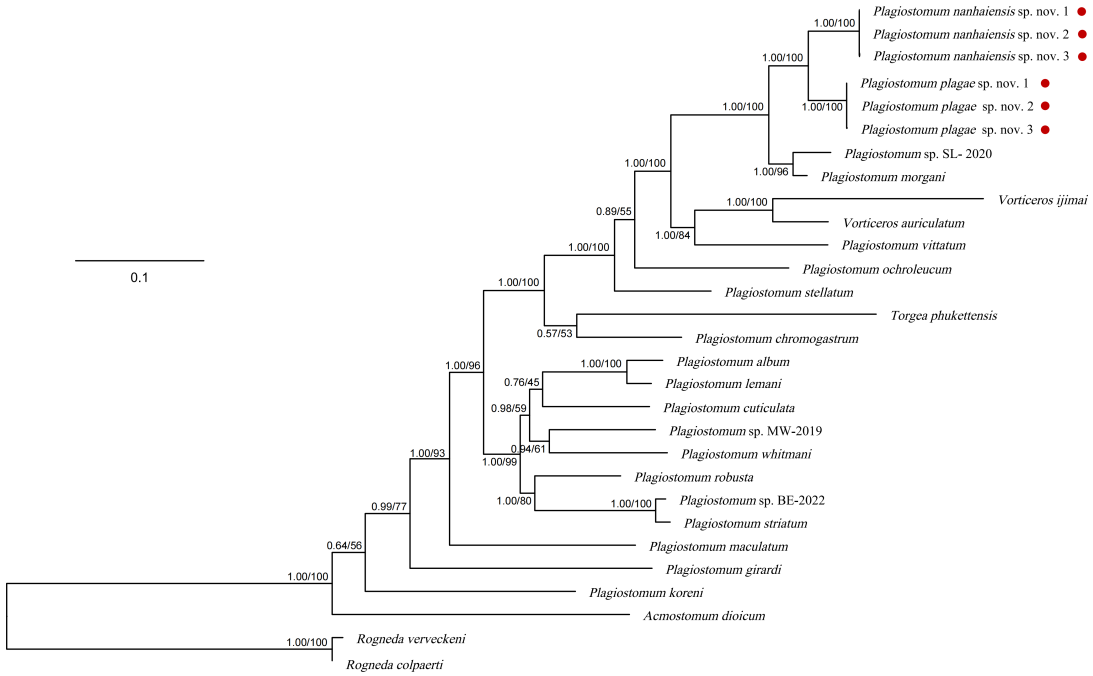

FIGURE 6
Phylogenetic tree based on concatenated sequences (*18S rDNA–28S rDNA*). The numbers at the nodes represent support values (posterior probability/bootstrap values). Red points: species from this study.

FIGURE 7
Hypodermic impregnation of *Plagiostomum nanhaiensis* sp. nov. **(A)** The flatworm extends its muscular penis. **(B)** The morphology of the penis during the fertilization process. **(C)** After fertilization, the flatworm retracts its penis. **(D)** An individual that has received sperm injects sperm into another individual. Scale bar, 50 µm. Arrow: Vesicula seminalis left after hypodermic impregnation.

the blunt penial papilla firmly anchors to the recipient, preventing escape during movement (Figure 7B). Throughout the mating process, the lower midsection of the injecting individual remains noticeably contracted, facilitating direct sperm injection into the recipient. After fertilization, the injecting individual retracts its penis (Figure 7C). Occasionally, the recipient's body contracts in response to the injection, resulting in the expulsion of sperm and the formation of a transparent sac-like protrusion while this phenomenon does not occur after every fertilization event (Figure 7D). In addition, we did not observe simultaneous bidirectional or multidirectional fertilization; there were instances where an individual that had just received sperm immediately became the injecting individual for another (Figure 7D).

3.4 Sex allocation

In natural habitats, the hermaphroditic reproductive structures of the two new species of flatworms remain stable (Figure 8A). However, during cultivation, with the increase of culture time and the decrease of group density, both species exhibit degeneration of the male reproductive organ. The initial signs of degeneration include shrinkage of the vesicula seminalis, which ceases to store sperm, while no significant changes were observed in the prostate gland cells. Additionally, the structure of the testis degenerates, resulting in a decreased sperm count and eventually disappearance of the penis. The penile sheath and the common atrium also show signs of atrophy (Figure 8B). In the later stages of degeneration, the vesicula seminalis, prostate gland cells, and penile sheath disappear, and the common atrium shrinks into a crevice, ultimately transforming into solid tissue (Figures 8C, D, G). During this process, the intestine and female reproductive structures remain intact (Figures 8B–F).

Our comparison of sex allocation in *P. nanhaiensis* sp. nov. between natural habitats and cultivation found that, among the 60 mature individuals of *P. nanhaiensis* sp. nov. collected from the wild, only two exhibited degeneration of the male reproductive organ, with 96.7% of individuals remaining hermaphroditic. In contrast, after 14 days of single, triad, and group cultivations, the percentages of hermaphroditic individuals increased to 40%, 55.6%, and 90%, respectively. Further observation revealed that the male reproductive organs of *P. nanhaiensis* sp. nov. degenerated completely after 10 to 21 days in the single cultivation (n = 10) and after 10 to 30 days in the triad cultivation (n = 21).

4 Discussion

4.1 Taxonomic status of two new species

Currently, the species identification of Plagiostomidae mainly relies on morphology and histology, with phylogenetic analysis as

10.3389/fmars.2025.1520497

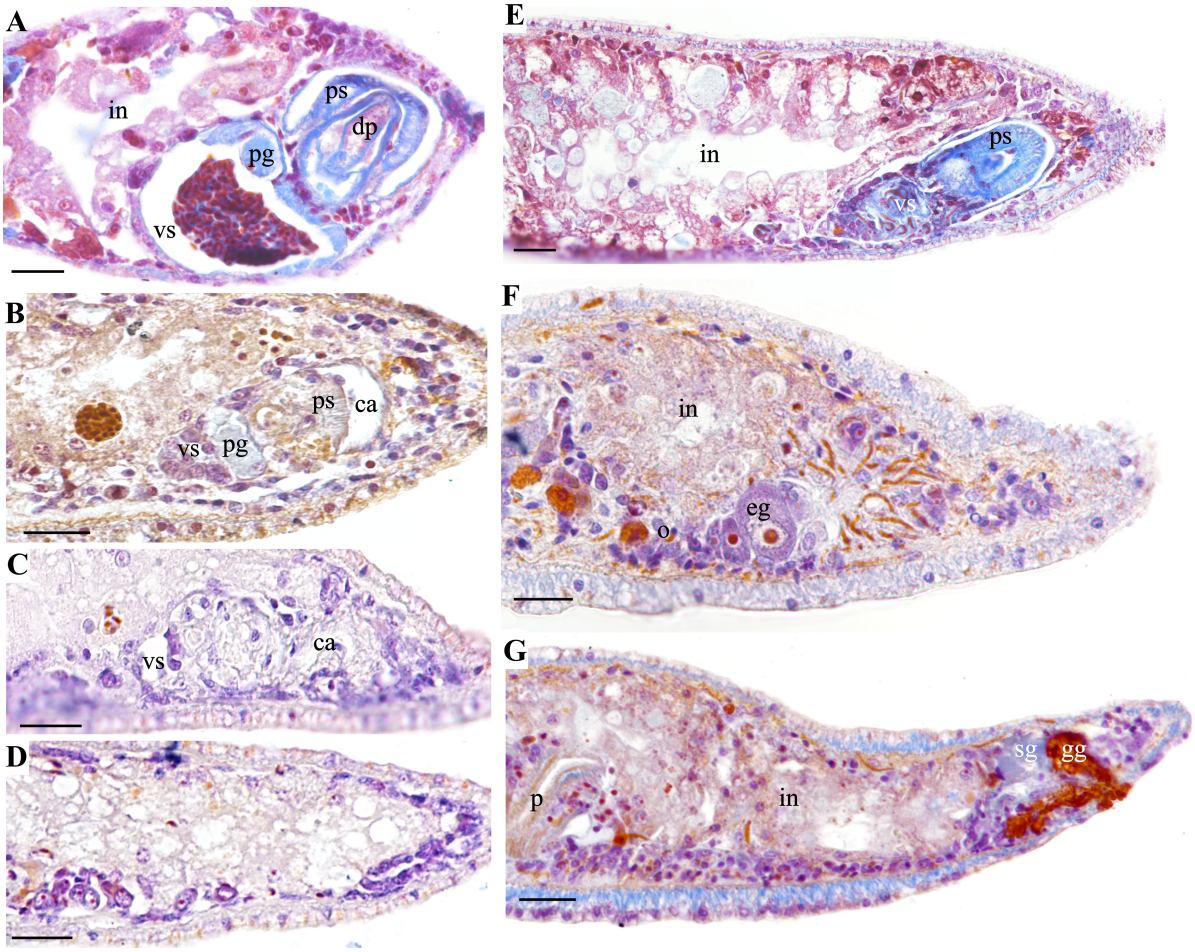

FIGURE 8
Comparison of male reproductive structure degeneration in *Plagiostomum plagae* sp. nov. and *Plagiostomum nanhaiensis* sp. nov. **(A–D)** *P. plagae* sp. nov. **(A)** Hermaphroditic stage in natural habitats. **(B)** Early stage of male reproductive structure degeneration. **(C)** Late stage of male reproductive structure degeneration. **(D)** Complete degeneration of male reproductive structures, with the ovaries remaining intact. **(E–G)** *Plagiostomum nanhaiensis* sp. nov. **(E)** Sagittal sections after 21 days of group cultivation, with male reproductive organs occupying a large space within the body. **(F, G)** Consecutive sagittal sections after 21 days of single cultivation, with male reproductive structures completely degenerated into solid tissue and female structures remaining intact. Scale bar, 25 μm.

asupplement. The two new species, *P. nanhaiensis* sp. nov. and *P. plagae* sp. nov., exhibit similarities in body size, life habits, juvenile characteristics, and egg development. However, they do not interbreed and display significant differences in pigmentation stripes and histological structures, indicating that they are two distinct species (Westram et al., 2022). Molecularly, the K2P distance among *Plagiostomum* species, based on *18S rDNA* and *28S rDNA* sequences, ranged from 2.2% to 22%. Although most distances exceed 10%, the genetic distance between three individuals of two species is approximately 0, and the genetic distance (5.4%) between *P. nanhaiensis* sp. nov. and *P. plagae* sp. nov. is similar to that between *P. morgani* Graff (5.3% and 6.5%, respectively), indicating clear genetic divergence. Meanwhile, phylogenetic analyses revealed that both *P. nanhaiensis* sp. nov. and *P. plagae* sp. nov. formed independent clades and were sister taxa to each other, exhibiting a certain evolutionary distance from other species. Based on the above evidence, we consider *P. nanhaiensis* sp. nov. and *P. plagae* sp. nov. to be two distinct new species.

4.2 Reproductive strategies of the two new species

To date, 85 species of *Plagiostomum* have been recorded, but little attention has been given to their mating behavior, egg-laying behavior, and individual development. A current study observed the mating behavior and individual developmental process of *P. robusta*, indicating that this species performs hypodermic impregnation (Wang et al., 2024). Therefore, we investigated the mating and egg-laying behaviors of *P. nanhaiensis* sp. nov. and *P. plagae* sp. nov. to further explore the biological characteristics and reproductive strategies of *Plagiostomum* species.

Hypodermic impregnation, being common in hermaphroditic animals, was considered as the response to sexual conflict allowing forced copulation, thereby increasing fertilization success, reducing sperm competition, and ensuring the survival of offspring (Ramm, 2017; Schärer and Janicke, 2009). The similar fertilization between *P. nanhaiensis* sp. nov., *P. plagae* sp. nov., and *P. robusta* indicated that most species in *Plagiostomum* may perform hypodermic

impregnation (Wang et al., 2024). Among flatworms, hypodermic impregnation was first discovered in *Macrostomum*, and their mating behavior, reproductive structures, and other characteristics have been extensively studied (Brand et al., 2022; Schärer et al., 2004, 2011). The species of *Macrostomum* have sharp bony penile stylets and simple sperm structures, allowing them to quickly pierce the body surface of their mate and inject sperm (Brand et al., 2022; Schärer et al., 2004, 2011). Although *P. nanhaiensis* sp. nov. and *P. plagae* sp. nov. exhibit different sperm structures, both are similarly simple (Figures 2, 5). Additionally, the copulatory organs of *P. nanhaiensis* sp. nov., *P. plagae* sp. nov., and *P. robusta* are fleshy penises, lacking needle-like or stylet structures, being different from *Macrostomum* (Brand et al., 2022; Schärer et al., 2004, 2011; Wang et al., 2024). Nevertheless, species of *Plagiostomum* can still anchor their mating partner using the penial papilla, allowing the penis to inject their sperms. Hypodermic impregnation species often exhibit self-fertilization when the mating partner is unavailable, which is commonly regarded as a safeguard mechanism for reproduction (Giannakara and Ramm, 2017; Janicke et al., 2016; Noël et al., 2017). Recent studies on *Macrostomum* have revealed that the initiation of self-fertilization not only is caused by the female's inability to receive sperm but also relates to the maintenance of male reproduction (Kaufmann and Schärer, 2020). During the cultivation of *P. nanhaiensis* sp. nov. and *P. plagae* sp. nov., we also observed their self-fertilization. Particularly, when multiple potential mates were present, *P. nanhaiensis* sp. nov. still exhibited self-fertilization behavior, further indicating that self-fertilization not merely is an emergency strategy triggered by specific environmental pressures (such as mate scarcity) but may be an inherent reproductive strategy.

Sex allocation is a critical reproductive strategy in hermaphroditic organisms, as it determines how resources are distributed between male and female functions to optimize reproductive success (Charnov, 1979, 1984; Fischer, 1981). However, accurately measuring these allocations in hermaphrodites is complex due to the need to quantify both male and female organs, considering both static and dynamic changes over time (Schärer, 2009). Currently, flatworms of the order Macrostomida are primarily assessed based on the relative proportions of sexual organs and glands to measure sex allocation (Brand et al., 2022; Janicke et al., 2013; Vellnow et al., 2018). Interestingly, during the cultivation of the two new species, we observed the complete degeneration of male reproductive structures, providing a clear indicator of female-only individuals. Complete feminization in hermaphrodites is rare and may represent an extreme sex allocation strategy.

Our cultivation revealed that the proportion of hermaphroditic individuals increased with the expansion of the group. Additionally, our observation of the flatworms collected from the wild in different seasons, from March to June and from October to November, showed that their hermaphroditic reproductive structures remained stable in the natural habitat. However, the male structures degenerated after the small-scale laboratory cultivation, indicating that seasonal changes and temperature fluctuations are not decisive factors for their sex allocation. Furthermore, in individuals with degenerated male reproductive structures, the intestine and other organ structures remained intact, ruling out the hypothesis that starvation was the cause of autophagy and organ disappearance. In summary, we suggested that sex allocation in flatworms is plastic, with mating group size being the most significant influencing factor corresponding to the traditional sex allocation theories (Charnov, 1984; Schärer, 2009). This phenomenon suggests that in natural environments, with the increase of mating group size, individuals tend to allocate more resources to male reproductive functions to overcome sexual selection pressures and to ensure reproduction during multiple male competition, thereby increasing the success probability of fertilization (Brand et al., 2022; Charnov, 1984; Janicke et al., 2013; Schärer, 2009). In contrast, in smaller or single-cultured conditions, the competing sperm are highly related. This leads to diminished returns on investment in sperm production, as producing additional sperm primarily results in competition among one's own sperm—a phenomenon known as local sperm competition (LSC) (Brand et al., 2022; Janicke et al., 2013). The LSC reduces the effectiveness of additional sperm investment, leading to a shift in resource allocation toward female reproductive functions and thus decreasing the level of sperm competition (Brand et al., 2022; Janicke et al., 2013). This strategy allows the individuals to adapt to the environment by increasing the quantity and quality of offspring when the mating opportunities are limited (Brand et al., 2022; Charnov, 1984; Janicke et al., 2013; Schärer, 2009). Compared to closed laboratory cultures, the group size of flatworms in natural habitats is larger, so the proportion of hermaphroditic individuals among mature flatworms collected from the wild is extremely high. This indicates that the evolution of sex allocation in flatworms is closely related to their social and environmental conditions and the sex allocation strategies exhibit adaptive changes under different ecological contexts.

4.3 Natural survival analysis of the two new species

Similar to those flatworms of the family Dugesiidae, the eggs of these two new species connect the egg stalk and base through mucus secreted by the reproductive glands (Solà et al., 2022). Their egg base adheres to the walls of the culture dish, which securely anchors the egg and reduces dispersion. In addition, the eggs undergo color change and hardening after being laid, which better protects the embryo inside the eggshell and improves the survival rate of the embryo. In addition to increasing embryo survival through egg fixation and eggshell hardening, flatworms also continuously collect and transport surrounding debris during and after egg-laying to cover the embryos, reducing the likelihood of predation by predators. The two new species in this study exhibit considerable similarity in diet, egg development, and juvenile morphology, indicating a trend of convergent evolution in the same habitat, with significant niche overlap and intense interspecies competition. However, during laboratory cultivation, slight differences in habitat preferences were observed between the two species: *P. nanhaiensis* sp. nov. often resides in the sediment, while *P. plagae* sp. nov. prefers to inhabit the side walls near the water surface. Multiple field collections have shown that *P. nanhaiensis* sp. nov. is more abundant than *P. plagae* sp. nov., indicating that *P. nanhaiensis* sp. nov. is the competitive dominant species between the two.

Data availability statement

The original contributions presented in the study are included in the article/Supplementary Material. Further inquiries can be directed to the corresponding authors.

Ethics statement

The manuscript presents research on animals that do not require ethical approval for their study.

Author contributions

LF: Data curation, Formal Analysis, Investigation, Methodology, Validation, Writing – original draft, Writing – review & editing. SZ: Data curation, Investigation, Writing – original draft. MT: Funding acquisition, Resources, Writing – review & editing. TS: Methodology, Resources, Supervision, Writing – review & editing. AW: Conceptualization, Supervision, Writing – review & editing.

Funding

The author(s) declare that financial support was received for the research, authorship, and/or publication of this article. This work was supported by the National Natural Science Foundation of China (grant no. 32303034).

Acknowledgments

We sincerely thank Mr. Yi-Tao Lin from Hong Kong Baptist University for providing valuable comments on this manuscript, Yuping Hong and Minjia Li from Shenzhen University for assistance with specimen collection and culture, and Xiang Xie from Shenzhen University for assistance with phylogenetic analysis.

Conflict of interest

The authors declare that the research was conducted in the absence of any commercial or financial relationships that could be construed as a potential conflict of interest.

Generative AI statement

The author(s) declare that no Generative AI was used in the creation of this manuscript.

Publisher's note

Supplementary material

The Supplementary Material for this article can be found online at: https://www.frontiersin.org/articles/10.3389/fmars.2025.1520497/full#supplementary-material

SUPPLEMENTARY FIGURE 1
Satellite map of the collection sites of *Plagiostomum nanhaiensis* sp. nov. and *Plagiostomum plagae* sp. nov., obtained from Google Earth. The collecting site is marked with a red star.

SUPPLEMENTARY TABLE 1
GenBank accession numbers of sequences for species taxa used in the phylogenetic analyses.

References

Brand, J. N., Harmon, L. J., and Schärer, L. (2022). Mating behavior and reproductive morphology predict macroevolution of sex allocation in hermaphroditic flatworms. *BMC Biol.* 20, 35. doi: 10.1186/s12915-022-01240-1

Capella-Gutierrez, S., Silla-Martinez, J. M., and Gabaldon, T. (2009). trimAl: a tool for automated alignment trimming in large-scale phylogenetic analyses. *Bioinformatics* 25, 1972–1973. doi: 10.1093/bioinformatics/btp348

Charnov, E. L. (1979). Simultaneous hermaphroditism and sexual selection. *Proc. Natl. Acad. Sci. United States America* 76, 2480–2484. doi: 10.1073/pnas.76.5.2480

Charnov, E. L. (1984). *The Theory of Sex Allocation* (Princeton: Princeton University Press).

Fischer, E. A. (1981). Sex allocation in a simultaneously hermaphroditic coral reef fish. *Am. Naturalist* 117, 64–82. doi: 10.1086/283686

Frey, H., and Leuckart, R. (1847). Beiträge zur Kenntnis wirbelloser Thiere: mit besonderer Berücksichtigung der Fauna des Norddeutschen Meeres. *Beiträge Zur Kenntnis Wirbelloser Thiere* 110–130. doi: 10.5962/bhl.title.2128

Gao, J., Wang, A. T., and Zhang, Y. (2011). Biological characteristics of *plagiostomum* (Prolecithophora, plagiostomidae). *Chin. J. Zoology.* 46, 8–15.

Giannakara, A., and Ramm, S. A. (2017). Self-fertilization, sex allocation and spermatogenesis kinetics in the hypodermically inseminating flatworm *Macrostomum pusillum*. *J. Exp. Biol.* 220, 1568–1577. doi: 10.1242/jeb.150995

Graff, L. V. (1911). Alocoela, Rhabdocoela und Alloeocoela des Ostens der Vereinigten Staaten: Mit Nachtüngen zu den marinen Turbellarien Orotavas und der Küste Europas. *Z. Für Wissenschaftliche Zoologie* 99, 68–65.

Graff, L. V. (1882). *Monographie der Turbellarien. (Vol. 1). W. Engelmann.*

Grosbusch, A. L., Bertemes, P., Kauffmann, B., Gotsis, C., and Egger, B. (2022). Do not lose your head over the unequal regeneration capacity in prolecithophoran flatworms. *Biology* 11, 1588. doi: 10.3390/biology11111588

Janicke, T., Marie-Orleach, L., De Mulder, K., Berezikov, E., Ladurner, P., and Schärer, L. (2013). Sex allocation adjustment to mating group size in a simultaneous hermaphrodite. *Evolution* 67, 3233–3242. doi: 10.1111/evo.12179

Janicke, T., Sandner, P., Ramm, S. A., Vizoso, D. B., Schärer, L., and Berezikov, E. (2016). Experimentally evolved and phenotypically plastic responses to enforced monogamy in a hermaphroditic flatworm. *J. Evolutionary Biol.* 29, 1713–1727. doi: 10.1111/jeb.12908

Jensen, O. S. (1878). *Turbellaria ad litora Norvegiae occidentalia. Turbellarier ved Norges Vestkyst*. 56–57.

Kalyaanamoorthy, S., Minh, B. Q., Wong, T. K. F., von Haeseler, A., and Jermiin, L. S. (2017). ModelFinder: Fast model selection for accurate phylogenetic estimates. *Nat. Methods* 14, 587–589. doi: 10.1038/nmeth.4285

Karling, T. G. (1940). Zur Morphologie und Systematik der Alloeocoela cumulate und Rhabdocoela lecithophora (Turbellaria). *Acta Zoologica Fennica*. 26, 1–260.

Karling, T. G. (1962). Marine turbellaria from the Pacific coast of North America. I. Plagiostomidae. *Arkiv för Zoologi* 15, 113–141.

Katoh, K., Rozewicki, J., and Yamada, K. D. (2019). MAFFT online service: Multiple sequence alignment, interactive sequence choice and visualization. *Briefings Bioinf.* 20, 1160–1166. doi: 10.1093/bib/bbx108

Kaufmann, P., and Schärer, L. (2020). Is the initiation of selfing linked to a hermaphrodite's female or male reproductive function? *Behav. Ecol. Sociobiol.* 74, 41. doi: 10.1007/s00265-020-02835-3

Kuraku, S., Zmasek, C. M., Nishimura, O., and Katoh, K. (2013). ALEAVES facilitates on-demand exploration of metazoan gene family trees on MAFFT sequence alignment server with enhanced interactivity. *Nucleic Acids Res.* 41, W22–W28. doi: 10.1093/nar/gkt389

Lanfear, R., Calcott, B., Ho, S. Y. W., Guindon, S., Moir, R., and Reeves, J. (2012). PartitionFinder: Combined selection of partitioning schemes and substitution models for phylogenetic analyses. *Mol. Biol. Evol.* 29, 1695–1701. doi: 10.1093/molbev/mss020

Ma, L. A., Rong, C. H., and Wang, A. T. (2014). A new record of *Enterostomula graffi* (Prolecithophora, Cylindrostomidae) in China. *Chin. J. Zoology.* 49, 244–252.

Nguyen, L. T., Schmidt, H. A., von Haeseler, A., and Minh, B. Q (2015). IQ-TREE: A fast and effective stochastic algorithm for estimating maximum-likelihood phylogenies. *Mol. Biol. Evol.* 32, 268–274. doi: 10.1093/molbev/msu300

Noël, E., Jarne, P., Glémin, S., MacGregor, H., David, P., and Glémin, S. (2017). Experimental evidence for the negative effects of self-fertilization on the adaptive potential of populations. *Curr. Biol.* 27, 237–242. doi: 10.1016/j.cub.2016.11.069

Rambaut, A. (2009). *FigTree. Tree figure drawing tool*. Available online at: http://tree.bio.ed.ac.uk/software/figtree/ (Accessed September 14, 2024).

Rambaut, A., Drummond, A. J., Xie, D., Baele, G., and Suchard, M. A. (2018). Posterior summarization in Bayesian phylogenetics using Tracer 1.7. *Systematic Biol.* 67, 901–904. doi: 10.1093/sysbio/syy032

Ramm, S. A. (2017). Exploring the sexual diversity of flatworms: Ecology, evolution, and the molecular biology of reproduction. *Mol. Reprod. Dev.* 84, 120–131. doi: 10.1002/mrd.22770

Ronquist, F., Teslenko, M., van der Mark, P., Ayres, D. L., Darling, A., and Höhna, S. (2012). MrBayes 3.2: Efficient Bayesian phylogenetic inference and model choice across a large model space. *Systematic Biol.* 61, 539–542. doi: 10.1093/sysbio/sys029

Schärer, L. (2009). Tests of sex allocation theory in simultaneously hermaphroditic animals. *Evolution* 63, 1377–1405. doi: 10.1111/j.1558-5646.2009.00669.x

Schärer, L., and Janicke, T. (2009). Sex allocation and sexual conflict in simultaneously hermaphroditic animals. *Biol. Lett.* 5, 705–708. doi: 10.1098/rsbl.2009.0043

Schärer, L., Joss, G., and Sandner, P. (2004). Mating behaviour of the marine turbellarian *Macrostomum* sp.: These worms suck. *Mar. Biol.* 145, 373–380. doi: 10.1007/s00227-004-1314-7

Schärer, L., Littlewood, D. T. J., Waeschenbach, A., Yoshida, W., and Vizoso, D. B.. (2011). Mating behavior and the evolution of sperm design. *Proc. Natl. Acad. Sci. United States America* 108, 1490–1495. doi: 10.1073/pnas.1013892108

Schärer, L., and Pen, I. (2013). Sex allocation and investment into pre- and post-copulatory traits in simultaneous hermaphrodites: The role of polyandry and local sperm competition. *Philos. Trans. R. Soc. London Ser. B. Biol. Sci.* 368, 20120052. doi: 10.1098/rstb.2012.0052

Schmidt, O. (1852). Neue Rhabdocoelen aus dem nordischen und dem Adriatischen Meere. *Sitzungsberichte Der Mathematisch-naturwissenschaftlichen Classe Der Kaiserlichen Akademie Der Wissenschaften* 9, 490–505.

Solà, E., Leria, L., Stocchino, G. A., Bagherzadeh, R., Balke, M., Daniels, S. R., et al. (2022). Three dispersal routes out of Africa: A puzzling biogeographical history in freshwater planarians. *J. Biogeography* 49, 1219–1233. doi: 10.1111/jbi.14394

(2006–2024). *World List of Turbellarian Worms: Acoelomorpha, Catenulida, Rhabditophora*. Plagiostomum vittatum *(Frey & Leuckart 1847) Jenssen 1878*. Available online at: https://www.marinespecies.org/turbellarians/aphia.php?p=taxdetails&id=142922 (Accessed 2024, 09, 12).

Vaidya, G., Lohman, D. J., and Meier, R. (2011). SequenceMatrix: Concatenation software for the fast assembly of multi-gene datasets with character set and codon information. *Cladistics* 27, 171–180. doi: 10.1111/j.1096-0031.2010.00329.x

Vellnow, N., Marie-Orleach, L., Zadesenets, K. S., and Schärer, L. (2018). Bigger testes increase paternity in a simultaneous hermaphrodite, independently of the sperm competition level. *J. Evolutionary Biol.* 31, 180–196. doi: 10.1111/jeb.13213

Vellnow, N., Vizoso, D. B., Viktorin, G., and Schärer, L. (2017). No evidence for strong cytonuclear conflict over sex allocation in a simultaneously hermaphroditic flatworm. *BMC Evolutionary Biol.* 17, 103. doi: 10.1186/s12862-017-0931-4

Wang, Y., Huang, J., Zhang, Y., and Wang, A. T. (2024). Molecular phylogeny and ethology of the family Plagiostomidae (Platyhelminthes, Prolecithophora), with integrative description of a new species, *Plagiostomum robusta* A. Wang, sp. nov. *Front. Mar. Sci.* 11. doi: 10.3389/fmars.2024.1332011

Westram, A. M., Stankowski, S., Surendranadh, P., and Barton, N. (2022). What is reproductive isolation? *J. Evolutionary Biol.* 35, 1143–1164. doi: 10.1111/jeb.14005

World List of Turbellarian Worms (2004). *marinespecies.org*. Available online at: http://www.marinespecies.org (Accessed September 12, 2024).

Xia, X. (2013). DAMBE5: a comprehensive software package for data analysis in molecular biology and evolution. *Mol. Biol. Evol.* 30, 1720–1728. doi: 10.1093/molbev/mst064

Xiang, C. Y., Gao, F., Jakovlić, I., Lei, H. P., Hu, Y., and Zhang, H. (2023). Using PhyloSuite for molecular phylogeny and tree-based analyses. *iMeta* 2, e87. doi: 10.1002/imt2.87

Yang, Y., Li, J. Y., Sluys, R., Li, W. X., Li, S. F., and Wang, A. T. (2020). Unique mating behavior, and reproductive biology of a simultaneous hermaphroditic marine flatworm (Platyhelminthes, Tricladida, Maricola). *Invertebrate Biol.* 139, e12282. doi: 10.1111/ivb.12282